Original Paper

Crystallization and viscosity of phosphate melts in the system $Na_2O-CaO-MgO-P_2O_5-Al_2O_3-TiO_2$

Peter Wange, Jürgen Vogel[1], Silke Knoche[2] and Christian Rüssel

Otto-Schott-Institut für Glaschemie, Friedrich-Schiller-Universität Jena, Jena (Germany)

Glasses in the system $Na_2O-CaO-MgO-P_2O_5-Al_2O_3-TiO_2$ were studied with respect to their crystallization and viscosity. Glasses in the metaphosphate range are composed of phosphate chains, and possess a comparably small tendency to crystallization. Here, $AlPO_4$ in a cristobalite-like modification and $Ca_2P_2O_7$ are formed. Glasses in the intermediate range between metaphosphate and invert glass structures are composed of smaller phosphate units and show higher crystal growth velocities as well as higher viscosities. Additions of MgO, Al_2O_3 and TiO_2 result in a strengthening of the glass network, and hence, increasing viscosities and a notably smaller tendency to crystallization.

1. Introduction

Phosphate glasses show a viscosity-temperature behaviour different from that of silicate glasses. At comparable network former/network modifier ratios, phosphate glasses exhibit notably lower viscosities [1]. By analogy, also the crystallization behaviour is different. In silicate glasses, controlled volume crystallization might be enabled by microphase separation and subsequent nucleation and crystal growth. This is scarcely possible in phosphate glasses because they usually do not exhibit phase separation. Phosphate glasses mostly crystallize from the surface [2], however, it is also possible to initiate volume crystallization by adding nucleating agents such as noble metals or zirconia to the glass batch. For this purpose, phosphate glasses in the invert glass range are most advantageous, however, also metaphosphate glasses are suitable. Using this strategy, the preparation of bioactive phosphate glass-ceramics has been enabled, as previously reported in [3 and 4]. Their chemical solubility and also their bioresorptivity can be adjusted by the chemical composition. The glasses which these glass-ceramics have been prepared from also show some interesting properties, especially with respect to their corrosion behaviour in slightly acidic and neutral solutions [5]. As recently reported in [5], also small changes in the chemical composition notably affect the corrosion behaviour. Here three composition ranges can be distinguished: the invert glass range ($[P_2O_5] < 41$ mol%), the metaphosphate range ($[P_2O_5] > 47$ mol%) and the range in between. The pronounced tendency to crystallization, however, is a strong limitation with respect to other applications. This paper provides a study on the viscosity-temperature dependency and the crystallization of phosphate glasses in the system $Na_2O-CaO-MgO-P_2O_5-Al_2O_3-TiO_2$ with compositions in the metaphosphate glass range and in the composition range between the invert glass and the metaphosphate glass range.

Received 17 February, revised manuscript 2 June 2004.

[1] Now with: Institut für Physikalische Hochtechnologie, Friedrich-Schiller-Universität Jena, Jena (Germany).

[2] Now with: SCHOTT AG, Mainz (Germany).

2. Experimental

Glasses in the system $Na_2O-CaO-MgO-P_2O_5-Al_2O_3-TiO_2$ were melted from the raw materials $Ca(PO_3)_2$, $Mg(PO_3)_2$, $Al(PO_3)_3$, Na_2CO_3, $Al(OH)_3$ and TiO_2 (anatase). Here, the metaphosphate range ($[P_2O_5] > 47$ mol%) and an intermediate range (41 mol% $< [P_2O_5] <$ 47 mol%) between invert and metaphosphate glass range were considered. The batch compositions are summarized in table 1. Some of the compositions were analytically controlled by inductively coupled plasma emission optical spectroscopy (ICP-EOS). The analytical compositions deviate from the batch compositions especially with respect to the P_2O_5 concentration.

Due to P_2O_5 evaporation during melting, the P_2O_5 concentration in the glass was approximately 10 % (relative) lower than in the batch. In order to measure viscosities at high temperatures, a rotation viscometer (Bähr 403, Bähr, (Germany)) was used. The viscosities were continuously measured as a function of the temperature. In the temperature range studied, crystallization did not occur. Glasses with strong tendency to crystallization could only be studied in a very limited temperature range. To study the crystallization behaviour, DTA profiles (Shimadzu DTA 5, Shimadzu (Japan)) of powdered glass samples (grain sizes 250 to 315 µm) were recorded. Here, T_g as well as the crystalliza-

Table 1. Glass compositions studied (in mol%)

sample	[Na_2O]	[K_2O]	[CaO]	[MgO]	[P_2O_5]	[Al_2O_3]	[TiO_2]	[SiO_2]	[B_2O_3]
A	16	–	22	8	47	5	2	–	–
B	8	8	22	6	45	6	5	–	–
C	14.9	1.9	7.3	8.6	–	0.5	–	58.6	8.2
D	15.6	–	10.9	–	–	1.2	–	72.3	–
E	19.6	–	24.1	–	52.1	4.2	–	–	–
F	19	–	23.4	–	52.3	4.0	1.3	–	–
G	19	–	11.4	12	52.3	4	1.3	–	–
H	18.4	–	10.6	12	52.5	3.9	2.6	–	–
I	20.3	–	25	–	47.8	4.4	2.5	–	–
K	19.5	–	23.7	4.3	52.5	–	–	–	–
L	18.2	–	22.1	4.1	53	–	2.6	–	–
M	20.6	–	30.6	–	40.9	5.5	2.4	–	–
N	16	–	26	4	47	5	2	–	–
O	12	4	18	8	47	6	5	–	–
P	15.7	–	25.5	3.9	46.1	4.9	3.9	–	–
R	10	6	20	6	45	6	5	2 ZnO	2 BaO
S	16	–	26	4	47	5	2	–	–

Table 2. Temperatures attributed to viscosities at 10 and 10^3 Pa s

sample	T_1 in °C	T_3 in °C	$T_1 - T_3$ in K
A	798	625	173
B	812	655	157
E	720	560	160
F	761	582	179
G	781	598	183
H	802	612	190
I	736	580	156
K	680	510	170
L	710	530	180
M	942	705	237
O	830	640	184

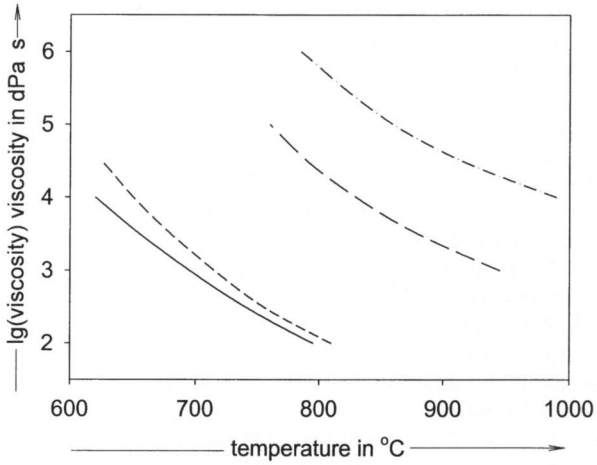

Figure 1. Viscosity-temperature dependency of two phosphate and two silicate glasses; —: sample A, – –: sample B, - - -: sample C, and —·—: sample D.

tion temperature (exothermic peak in the DTA profile) were observed. To determine crystal growth velocities, small glass samples were thermally treated in a gradient furnace and subsequently the crystal sizes were determined in an optical microscope. In all samples, mainly surface crystallization was observed. The experimental parameters (time and temperature range) had to be adjusted to the respective glass compositions. The experimental error in the crystal growth velocity was ± 10 %.

3. Results and discussion

3.1 Viscosities

Figure 1 presents viscosities in the range of 10 to $10^{3.5}$ Pa s of two phosphate glasses (samples A and B) and two silicate glasses (samples C and D). The composition of sample A is in the metaphosphate range and that of sample B between the metaphosphate and the invert glass range. The highest viscosities at all temperatures studied are those of sample D, a silicate glass with a composition comparable to a float glass. Sample C possesses somewhat lower viscosities than sample D. It has a composition typical of a bioresorbable fibre glass for thermal insulating composites. The two phosphate glasses have much lower viscosities than the silicate glasses. Here, sample A possessing a P_2O_5 concentration of 47 mol% has lower viscosities than sample B (45 mol% P_2O_5). Glass A lies in the metaphosphate range, while glass B is attributed to the intermediate composition range. Both glasses also contain TiO_2 and Al_2O_3, which are incorporated as AlO_4 and TiO_6 units and interconnect the phosphate chains to a certain extent. In the metaphosphate glass (sample A) the viscosity is lower, although the phosphate chains should be longer than in sample B. The effect of TiO_2 on the viscosity is illustrated in figure 2. Sample E does not contain TiO_2 while sample F contains 1.3 mol% TiO_2. The molar ratios of the other melt components are kept constant. The comparably small TiO_2 concentration leads to viscosities around four times higher than those of the glass without titania. The viscosity-temperature curve is shifted around 40 K to higher temperatures in the titania containing glass. Samples G and H possess titania concentrations of 1.3 and 2.6 mol%. Also here, the molar ratios of the other melt components were kept constant. The sample with the larger TiO_2 concentration possesses the higher vis-

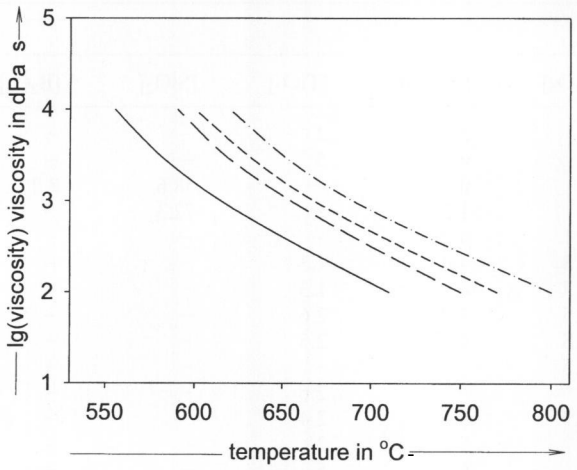

Figure 2. Viscosity-temperature dependency of some phosphate glasses; —: sample E, =—: sample F, - - -: sample G, and —·—: sample H.

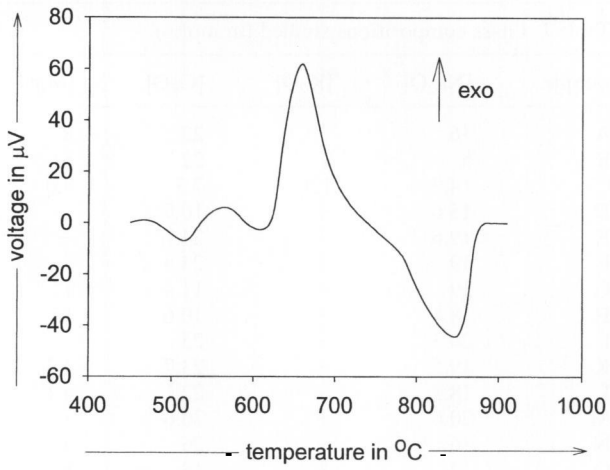

Figure 3. DTA profile of sample M (heating rate 10 K/min).

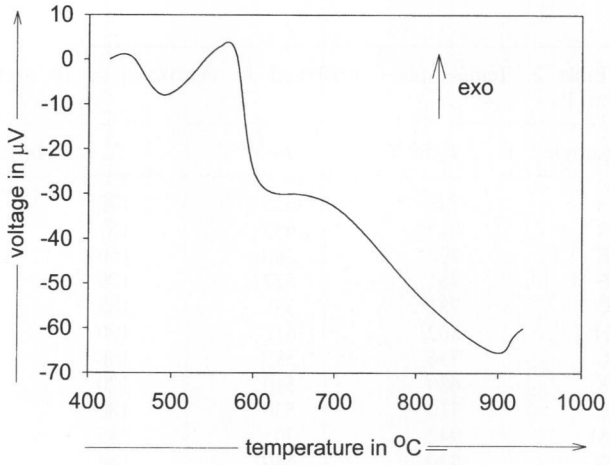

Figure 4. DTA profile of sample A (heating rate 10 K/min).

cosities. The effect is not as pronounced as in sample E and F. The viscosity-temperature curve is shifted by around 20 K to higher temperatures. Sample G and F possess the same molar TiO_2 concentration, however, sample F contains 12 mol% MgO and 11.4 mol% CaO, while sample G contains 23.4 mol% CaO and does not contain any MgO. The sum of the molar alkaline earth concentrations as well as the molar concentrations of all other components are the same. It is seen that a partial substitution of MgO for CaO leads to an increase in viscosity. The effect is clearly significant, the viscosity-temperature curve is shifted around 20 K to higher temperatures. It should be noted that in all compositions shown in figure 2, an increase in viscosity also results in an increase in the workability range. This can be illustrated by the difference of the temperatures attributed to viscosities of 10 and 10^3 Pa s. These differences are 160, 179, 183 and 190 K for the samples E, F, G and H, respectively. Table 2 shows viscosities at 10 and 10^3 Pa s of all glass compositions studied. The results can be summarized as follows: decreasing P_2O_5 concentrations led to an increase in the viscosities, this is especially illustrated by the sample M which has the lowest P_2O_5 concentration of all samples studied (40.9 mol%). The incorporation of Al_2O_3 or TiO_2 leads to an increase in viscosity as well as the replacement of CaO by MgO. The largest workability range ($T_1(\eta = 10\ \text{Pa s}) - T_3(\eta = 10^3\ \text{Pa s}) = 237\ \text{K}$) is observed at the composition M.

It has already been reported [6 and 7] that phosphate units, especially Q^0 and Q^1 units, are joined by AlO_4^- and TiO_6^{2-} polyhedra. This leads to a stabilization of the glass structure, which results in increasing viscosities. The replacement of CaO by MgO has the same effect (as shown above): it joins the phosphate units, while Ca^{2+} acts as network modifier which increases the number of nonbridging oxygens.

3.2 Crystallization

In figures 3 and 4, DTA profiles of the samples M and A are respectively shown. In sample M which has an invert glass structure, two strong exothermic peaks at temperatures of around 550 and 680 °C are seen. This is a hint of the formation of two different crystalline phases. As proved by XRD, in this case, $AlPO_4$ (in cristobalite-like structure) is the phase formed first. At higher temperatures, additionally $Ca_2P_2O_7$ is formed. In the DTA profile of sample A (see figure 4), two exothermic peaks at 560 and 660 °C are observed. Sample A is a glass in the metaphosphate range and does not show as intense exothermic peaks as sample M. The observed peaks are attributed to the formation of the same crystalline phases ($AlPO_4$ and $Ca_2P_2O_7$). In the case of invert glass structures, the crystal growth velocities were too large to be studied in the entire temperature range using conventional tempering techniques. This was also due to the large crystal density, caused by a large nucleation rate. In the metaphosphate range, the determination of crystal growth velocities using this technique, however, was possible. In figure 5, crystal growth velocities of the sample R are shown as a function of temperature for the two crystalline phases formed. On all samples surface crystallization was observed. The phases formed can clearly be distinguished in optical micrographs as shown in figures 6 and 7: $AlPO_4$ in cristobalite-like modification forms cubic crystals (see figure 6), while $Ca_2P_2O_7$ occurs as dentrites. The maximum in the crystal growth velocity of $AlPO_4$ is ob-

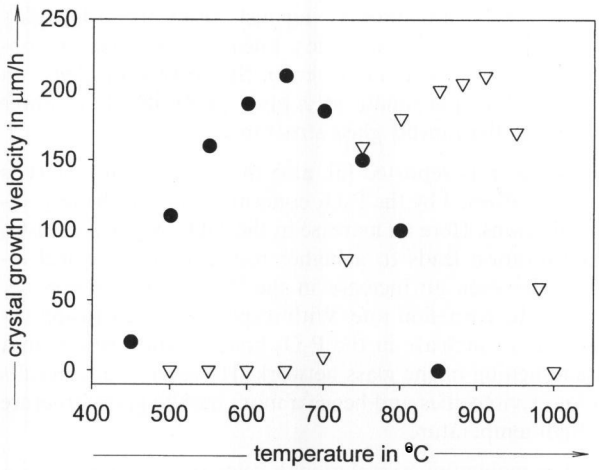

Figure 5. Crystal growth velocity of sample R as a function of temperature; ●: $AlPO_4$ (cristobalite-like modification), and ▽: $Ca_2P_2O_7$.

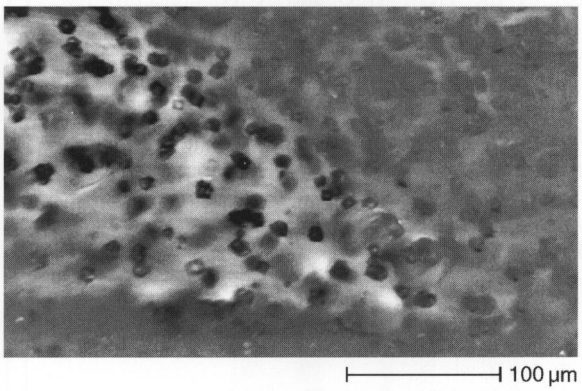

Figure 6. Optical micrograph of sample P after tempering at 800 °C for 0.5 h. The cubic crystals are $AlPO_4$.

served at 650 °C. At higher temperatures, the crystal growth velocity strongly decreases and becomes negligible at 850 °C. The crystallization of $Ca_2P_2O_7$ occurs at higher temperatures and is maximum at 910 °C. The maximum is fairly broad, the crystal growth velocities at 800 and 950 °C are only around 12 % lower than at 910 °C. At the maxima both crystal growth velocities are 210 µm/h. Figure 8 presents crystal growth velocities of the sample S. Also here, $AlPO_4$

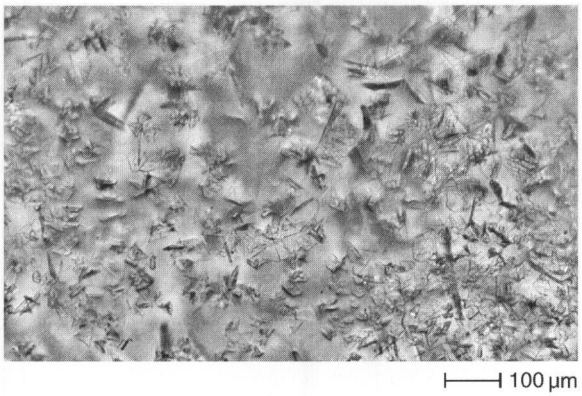

Figure 7. Optical micrograph of sample R after tempering at 950 °C for 1 h. The crystalline phase is $Ca_2P_2O_7$.

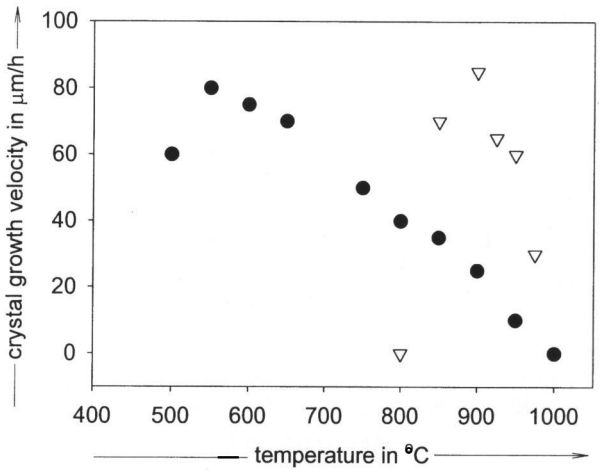

Figure 8. Crystal growth velocity of sample S as a function of temperature; ●: $AlPO_4$ (cristobalite-like modification), and ▽: $Ca_2P_2O_7$.

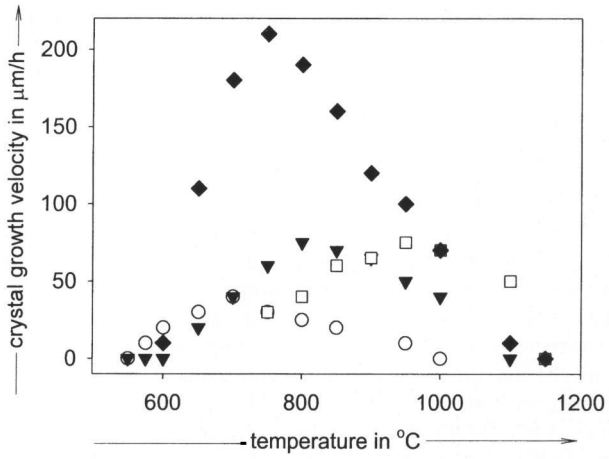

Figure 9. Crystal growth velocities as a function of the temperature; ○: sample A, ◆: sample B, ▼: sample O, and □: sample P, crystal phase: $AlPO_4$ (cristobalite-like modification).

as well as $Ca_2P_2O_7$ crystallizes. The maximum crystal growth velocity of $AlPO_4$ is observed at 550 °C. $Ca_2P_2O_7$ crystallizes at higher temperatures, the attributed maximum is observed at 900 °C. The maximum values of the crystal growth velocities are 80 and 85 µm/h and hence notably smaller than those of sample R.

In figure 9, crystal growth velocities (crystal phase: $AlPO_4$ (cristobalite-like modification) of samples A, B, O and P are shown. The samples A and O have the same P_2O_5 concentration (47 mol%), while that of sample P is slightly smaller (46.1 mol%). These samples show maxima in the crystal growth velocity of 700, 800 and 950 °C, respectively. They all lie in the range of 40 to 75 µm/h. Sample A possesses the smallest TiO_2 concentration and shows the maximum at the lowest temperature. Sample P has a larger TiO_2 concentration (4 mol%) and 4 % CaO are replaced by MgO. Here, the maximum is shifted to considerably larger temperatures (950 °C). In comparison to sample A, sample O has a larger Al_2O_3 concentration (6 mol%) and 4 % Na_2O are replaced by K_2O, which also leads to a shift in the maximum to higher temperatures. Sample B has the smallest

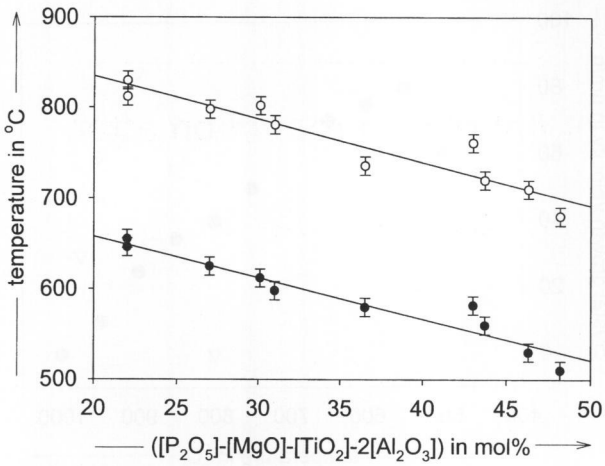

Figure 10. Temperatures attributed to the viscosities of 10 (○) and 10^3 Pa s (●) as a function of $[P_2O_5]$-[MgO]-2$[Al_2O_3]$-$[TiO_2]$ (in mol%).

P_2O_5 concentration and shows the highest crystal growth velocities.

From figures 5, 8 and 9, it can be concluded that the maximum crystal growth velocity strongly depends on the P_2O_5 concentration. For 45 mol% P_2O_5, it is around 200 µm/h and drops to 40 to 85 µm/h for 47 mol% P_2O_5. It should be noted that the increase in the P_2O_5 concentration leads to a decrease in viscosity. That means, the higher crystal growth velocities are observed in the glass with the higher viscosity. The concentrations of MgO, Al_2O_3 and TiO_2 are of minor importance for the maximum crystal growth velocity, however, they determine at which temperature the maximum occurs. With increasing Al_2O_3 and TiO_2 concentrations the maximum is shifted to higher temperature, while MgO seems to have the opposite effect. The dominating effect of Q^1 units in the invert glasses favours the crystallization, also because of the occurrence of Al−O−P bonds. Here, the crystallization of $AlPO_4$ occurs.

3.3 General remarks

The viscosity-temperature dependence of glasses in the system studied is strongly affected by the P_2O_5 concentration and components such as Al_2O_3, TiO_2 and MgO. While increasing P_2O_5 concentrations lead to decreasing viscosities, the addition of Al_2O_3, TiO_2 or MgO has the opposite effect. In figure 10, the temperatures attributed to viscosities of 10 and 10^3 Pa s are plotted against $[P_2O_5]$-$[TiO_2]$-[MgO]-2$[Al_2O_3]$. For both viscosities, linear correlations are obtained. Within the limits of error, the correlation lines run parallel. Metaphosphate structures generally show lower viscosities than invert glass structures.

As recently reported [5], also the chemical durability is strongly affected by the P_2O_5 concentration and the respective additions. Here an increase in the TiO_2, MgO and Al_2O_3 concentration leads to a higher resistance to chemical attack. However, an increase in the P_2O_5 concentration decreases the corrosion rate. With respect to the corrosion behaviour, an increase in the P_2O_5 concentration results in a strengthening of the glass network. However, it also results in lower viscosities and hence a more mobile glass structure at high temperatures.

The maximum crystal growth velocity decreases with increasing P_2O_5 concentration. This is a surprising effect, since increasing P_2O_5 concentrations lead to a lower viscosity, and hence also should lead to higher crystal growth velocities. While the crystal growth velocity is scarcely affected by the TiO_2, MgO and Al_2O_3 concentrations, the P_2O_5 concentration strongly affects the crystallization behaviour. If it is decreased by only 2 mol%, the crystal growth velocity drops by around the factor 3. This is of special importance for the preparation of glass-ceramics. Especially with respect to the evaporation of P_2O_5 during melting, special attention has to be paid to the homogeneity of the melt.

4. References

[1] Scholze, H.: Glass. Nature, structure and properties. Berlin et al.: Springer, 1991. P. 164 ff.

[2] Vogel, W.: Glaschemie. 3rd ed. Berlin et al.: Springer, 1992. P. 319 ff.

[3] Vogel, W.; Höland, W.: The development of bioglass ceramics for medical applications. Angew. Chem. Int. Ed. Engl. **26** (1987) pp. 527–544.

[4] Höland, W.; Wange, P.; Naumann, K. et al.: Control of phase formation processes in glass-ceramics for medicine and technology. J. Non-Cryst. Solids **129** (1998) pp. 152–162.

[5] Vogel, J., Wange, P., Knoche, S. et al.: Chemical solubility of phosphate glasses in the system Na_2O-CaO-MgO-P_2O_5-Al_2O_3-TiO_2 in aqueous solutions of different pH-values. Glass Sci. Technol. **77** (2004) pp. 82–87.

[6] Schtin, S.; Slemichin, S.: The structural part of Ti in K-Al-phosphate glasses. (Orig. russ.) Fiz. Khim. Stekla **5** (1979) pp. 171–177.

[7] Perry, C.; Knizer, D.: Magnetic exchange between Ti^{3+} ions in titanium phosphate glass. J. Appl. Phys. **50** (1979) pp. 1601–1603.

E404P004

Contact:

Prof. Dr. C. Rüssel
Otto-Schott-Institut für Glaschemie
Friedrich-Schiller-Universität Jena
Fraunhoferstraße 6
D-07743 Jena
E-mail: ccr@rz.uni-jena.de